

PREDICTION OF IMPACT SOUND TRANSMISSION OF LIGHTWEIGHT FLOORS

J Brunskog Engineering Acoustics, LTH, Lund University, Lund, Sweden
P Hammer Engineering Acoustics, LTH, Lund University, Lund, Sweden

1. INTRODUCTION

The interest in lightweight building techniques has increased during the last few years. However, it is well-known that this type of structures has poor impact sound insulation. Raised demands regarding sound insulation has lead to a development of lightweight floor structures and an acceptable impact sound insulation has been achieved, but still to a rather high production cost. In developing and explaining structures that have an acceptable insulation, a prediction model is an important tool. A prediction model for the impact noise can be said to consist of a chain in three parts: excitation - system - response. This paper is built on the report [1], and has partly been presented in [2].

2. THE EXCITATION

The ISO standard tapping machine applied on high impedance homogenous structures has been studied by e.g. Cremer and Heckl [3], Lindblad [4] and Vér [5]. Generally, a lightweight floor structure can not be seen as a high impedance homogenous structure. The structure is built up by thin plates of e.g. wood, chipboard or gypsum, and is reinforced by beam stiffeners. Thus, it can not generally be assumed that the force spectrum in [3-5] can be used.

The ISO standard tapping machine consists of five hammers, spaced equally along a line of 40 cm. However, as an approximation, it can be assumed that all impacts are located to a single position. Each hammer has a mass of $M=0.5$ kg and is dropped from a height h of 4 cm. The hammers strike the floor with a rate of $f_r=10$ times per second, giving a repetition time of $T_r=1/f_r=0.1$ s. However, consider initially a single hammer impact with a force time history $f_1(t)$. The Fourier spectrum for this force pulse is $F_1(f)=F_t(f_1(t))$, $F_t(\cdot)$ being the temporal Fourier transform operator (time to frequency). The excitation caused by the tapping machine can be seen as an array of force pulses $f_1(t)$. The time history of the repeated force $f_R(t)$ is

$$f_R(t) \equiv \sum_{n=-\infty}^{\infty} f_1(t - nT_r) = \sum_{n=-\infty}^{\infty} F_n e^{i2\pi nt/T_r}. \quad (1)$$

This time history is a periodic signal. Thus, the time history can be represented by a Fourier series, e.g. a two-sided complex Fourier series as shown in the second identity. The signal is represented by a series consisting of an infinite number of discrete frequency components with amplitude F_n .

$$F_R(f) = F_t(f_R(t)) = \sum_{n=-\infty}^{\infty} F_n \delta(f - nf_r). \quad (2)$$

where $F_R(f)$ denotes the spectrum of the repeated signal, and will be used in the next section as the excitation force of the system. Each amplitude is given by

$$F_n = \frac{1}{T_r} \int_0^{T_r} f_1(t) e^{-i2\pi nt/T_r} dt \quad (3a)$$

where $f_1(t)$ is the force time history of a single hammer impact. This integral is identical with the Fourier transform of the single force pulse except for the factor $1/T_r$. Thus, for the tapping machine

the repeated force components F_n is 10 s^{-1} times the force spectrum for a single impact. For low-frequency components the force pulse is usually short compared to the period of interest. Then, during the effective length of the force pulse, $\exp(-2\pi mt/T_r) \approx 1$, and the Fourier amplitude of the force pulse train can be approximated by

$$F_n|_{f \rightarrow 0} = \frac{1}{T_r} \int_0^{T_r} f_1(t) dt, \quad (3b)$$

which is identical with the mechanical impulse divided by T_r . The mechanical impulse equals the change in momentum. The hammer hits the slab with a velocity $v_0 = (2gh)^{1/2} = 0.886 \text{ m/s}$. If the impact is purely elastic, the momentum of the hammer after impact will be equal in magnitude but with the opposite sign as compared to before impact, i.e. the hammer will lift from the slab with the velocity v_0 . Thus, $F_n|_{f \rightarrow 0} = 2Mv_0/T_r = 7.087 \text{ N}$. This is the highest possible low-frequency asymptote of the impact spectrum, and thus the maximum value of the magnitude of the spectrum. Going to the other extreme, if the impact is so very damped that the entire momentum is dissipated during the impact, the hammer will not rebound. Then the mechanical impulse reads $F_n|_{f \rightarrow 0} = Mv_0/T_r = 3.544 \text{ N}$. This is the lowest possible low-frequency asymptote of the impact spectrum. Thus, the low-frequency asymptote has a span of 3.543 N, or 6 dB.

2.1 IMPACT FORCE, LUMPED SYSTEM DESCRIPTION

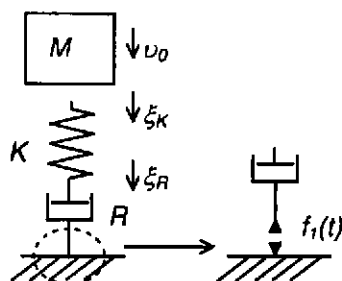


Figure 1 Model of hammer impact

A somewhat more realistic description than an elastic impact is to use a lumped model. The model and the solution used herein are taken from Lindblad [4]. A lumped model of the hammer impact on a floor can be seen in Figure 1. The floor consists of a resilient part and an energy consuming part, represented by a spring K and a dashpot resistance R respectively.

When the hammer has reached the slab, the differential equation for the assumed system together with the initial condition v_0 , and assuming frequency independent K and R , gives the solution [4]

$$f_1(t) = \begin{cases} \frac{v_0 K e^{-\frac{K}{2R}t} \sinh(\Omega_{oc}t)}{\Omega_{oc}}, & KM \geq 4R^2, \Omega_{oc} \equiv \sqrt{(K/2R)^2 - K/M} \\ \frac{v_0 K e^{-\frac{K}{2R}t} \sin(\Omega_{uc}t)}{\Omega_{uc}}, & KM < 4R^2, \Omega_{uc} \equiv \sqrt{K/M - (K/2R)^2} \end{cases}, \quad (4)$$

depending on whether the oscillation is over-critical or not. As the force reaches the zero crossing at t_{cross} , the hammer rebounds, takes off from the slab and is picked up by a catching mechanism. Thus, the force is zero henceforth. In the over-critical case the force will never completely be zero. However, the force still decreases rapidly after maximum, and is approximately zero at T_r . Each amplitude in the tonal spectrum is now given by (3 a), where the integration stops at $T_r \rightarrow \infty$ in the case of over-critical damping and $T_r \rightarrow t_{cross}$ in the case of under-critical damping. The time of zero-crossing is $t_{cross} = \pi/\Omega_{uc}$. Fourier transform over time to angular frequency ω of equation (5),

$$F_{1,over} = \frac{v_0 KM}{K - \omega^2 M + i\omega KM/R}, \quad F_{1,under} = v_0 KM \frac{1 + e^{-\frac{\pi}{\Omega_{uc}}(i\omega + \frac{K}{2R})}}{K - \omega^2 M + i\omega KM/R}, \quad (5a-b)$$

The low-frequency asymptote is

$$F_{i,over}|_{f \rightarrow 0} = v_0 M, \quad F_{i,under}|_{f \rightarrow 0} = v_0 M \left(1 + e^{-\frac{K}{2R} \frac{\pi}{\omega}} \right) \quad (5 \text{ c-d})$$

where (9 d) has two extremes depending on the resistance R ,

$$F_{i,under}|_{f \rightarrow 0, R \rightarrow \infty} = v_0 M 2, \quad F_{i,under}|_{f \rightarrow 0, R \rightarrow \frac{1}{2} \sqrt{KM}} = v_0 M, \quad (5 \text{ e})$$

agreeing with the asymptotes schematically derived in section 2.1 by means of the mechanical impulse and the change in momentum.

A suitable stiffness K and a resistance R have to be found to give a complete approximation of the impact description. In many cases the resilient part is due to an elastic surface layer on an otherwise stiff slab. The stiffness is then $K=EA_h/d$, e.g. V  r [5], where E is the Young's modulus and d is the thickness of the elastic layer, and A_h is the area of the hammer. The resistance is then related to local dissipation, $R=\eta(KM)^{1/2}$, η being the loss factor for the material. However, in the lightweight floor structures considered in this paper, the hammer hits a rather thin plate made of gypsum or wooden material. It can then be assumed that the resilient part is due to local deformation of the plate, and the resistive part is due to energy transportation in the plate. As a first approximation, the stiffness of the local deformation can be found in e.g. [6],

$$K = \frac{ED_h}{1 - \nu^2}, \quad (6)$$

where D_h is the diameter of the hammer. This local stiffness is found for a rigid stamp on a semi-infinite elastic solid, the so-called Bossinesq deformation. The resistance is taken as the real input impedance of a thin plate,

$$R = 8\sqrt{m'l'E}, \quad (7)$$

taking into account that energy is transported away from the excitation point by bending wave motion. Both of these lumped parameters are frequency independent, which is a necessary condition for the solution technique in the present section.

2.2 IMPACT FORCE, GENERAL SYSTEM DESCRIPTION

In section 2.1 the impact force spectrum was derived for frequency-independent parameters K and R in a mechanical series. The spectrum was given explicit expressions (5 a-b). However, the floor system can not generally be described by means of frequency-independent parameters. A more accurate description would be e.g. to calculate the driving point mobility from the system description.

However, the methods used in section 2.1 can not be used for a frequency-dependent mobility. Thus, an approach for finding the force spectrum for an arbitrary input mobility has to be found. The approach is to solve the differential equations in the frequency domain, inverse transform the result to find the time of rebound, and then transform the remaining force to the frequency range. In Figure 2 a) a more general model of the impact is shown.

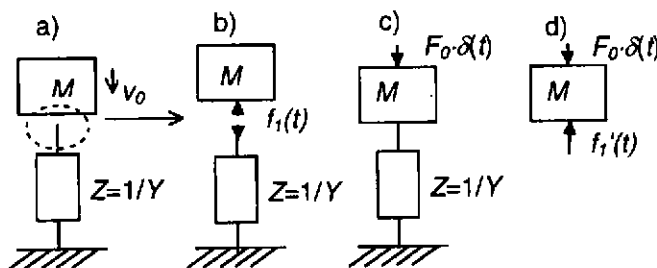


Figure 2 Modified impact description

This time the floor is described by a general input mobility Y (or impedance Z). The desired force, $f_1(t)$, is shown in Figure 2 b). To deal with this problem, consider instead Figure 2 c). The mass M is now fixed on top of the impedance Z . The entire system is driven by a force $F_0 \alpha(t)$. This modified problem is linear and time invariant. The equation of motion and the floor reaction force, if

taken in the frequency domain, is used and solved for impact force and velocity,

$$F_1' = \frac{F_0}{1 + i\omega MY}, \quad v = \frac{YF_0}{1 + i\omega MY} \quad (8)$$

where $v = F_1'(v(t))$ is the velocity spectrum of the floor and F_1' is the spectrum of the continuing impact force, i.e. the floor reaction force between the mass and the impedance in Figure 2 c-d), $F_1' = F_1'(f_1(t))$. The magnitude of the force F_0 has to be chosen so that the velocity at $t=0_+$ equals the velocity of the falling hammer. At $t=0_-$ the velocity should be zero. However, when evaluating $v(0)$ numerically, the evaluation is exact on zero, giving a value between $v(0_+)$ and $v(0_-)$, $v(0) = v_0/2$. The velocity of the floor at $t=0$ is evaluated as the integral over all frequencies,

$$v(0) = \frac{1}{2\pi} \int_{-\infty}^{\infty} v(\omega) d\omega = F_0 \frac{1}{2\pi} \int_{-\infty}^{\infty} \frac{d\omega}{i\omega M + 1/Y(\omega)} = F_0 I_0, \quad (9)$$

where equation (15 b) was used in the last equality. The integral I_0 is to be calculated numerically. Put (16) in to (17) to get the magnitude of the driving force in the modified system. Equation (15 a) then becomes

$$F_1' = \frac{v_0}{(1 + i\omega MY) 2I_0} \quad (10)$$

The time history of this force is found by an inverse Fourier transform, numerically implemented as a fast digital inverse transform. The moment of time for the first zero crossing of the force has then to be found. The actual, interrupted, excitation impact force then is $f_1(t) = f_1'(t) \cdot \theta(t - t_{cross})$, and the corresponding force spectrum is found using a Fourier transform,

$$F_1 = F_1'(f_1(t)), \quad F_n = F_1(nf_r) \cdot f_r, \quad (11)$$

numerically implemented as a fast digital transform. The Fourier series components F_n of (3 a) is then also found.

3. THE SYSTEM

3.1 DESCRIPTION OF THE SYSTEM

Consider a system of two coupled parallel plates of infinite extent separated by a cavity depth d , and with coupling through a cavity and through a rigid mechanical connection. The plates are modelled as classic thin plates. An excitation force acts on the upper plate, plate 1. Reaction forces from a periodic arrays of discontinuities in the form of beam stiffeners and from the surroundings and from cavity fluids are also present. The fluids satisfy the ordinary acoustic wave equation. The formulation will be a combination of Mace [7] and Lin and Garrelick [8]. A similar formulation can also be found in [9].

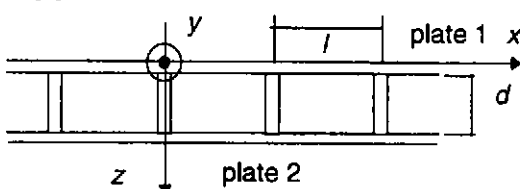


Figure 3 Floor system and co-ordinates.

Consider Figure 3. The first plate is excited by a pressure $p_e(x, y)e^{i\omega t}$ and is reinforced by parallel beams with a spacing l . The time variation $e^{i\omega t}$ will henceforth be suppressed throughout. The Cartesian co-ordinates and the beam spacing are defined in Figure 3.

The equations that we have to solve can be written as

$$\begin{cases} D_1 \nabla^4 w_1 - m_1'' \omega^2 w_1 = p_e + p_r - p_{t1} - p_c, \\ D_2 \nabla^4 w_2 - m_2'' \omega^2 w_2 = p_c - p_t + p_{t2} \end{cases}, \quad \nabla^4 = \left(\frac{\partial^2}{\partial x^2} + \frac{\partial^2}{\partial y^2} \right)^2, \quad (12)$$

The displacement of the plates in the positive z -direction, $w_1(x, y)$ and $w_2(x, y)$, satisfies the equation (12). The excitation pressure is p_e and the remaining reaction pressures are due to: fluid interaction

with the surrounding medium (transmission p_t and radiation p_r), the framing beams p_b and the coupling between the plates governed by a cavity p_c . Mass densities of the plates per unit area are denoted m''_1 and m''_2 respectively, and the flexural rigidity is denoted D_1 and D_2 respectively. Effects of moments and boundaries are of no concern. Passive, linear and small pressures and deformations are assumed.

The Fourier transform of w with respect to the co-ordinates x and y and the corresponding inverse transform is defined as

$$\tilde{w}_i(\alpha, \beta) = \int_{-\infty}^{\infty} \int_{-\infty}^{\infty} w_i(x, y) e^{i(\alpha x + \beta y)} dx dy, \quad w_i(x, y) = \frac{1}{4\pi^2} \int_{-\infty}^{\infty} \int_{-\infty}^{\infty} \tilde{w}_i(\alpha, \beta) e^{-i(\alpha x + \beta y)} d\alpha d\beta. \quad (13)$$

where α and β are the transform wavenumbers in the plate in the x - and y -directions, respectively. The continuity equation at each plate-frame connection points are assumed to be rigid and takes the following form

$$w_1(nl, y) = w_2(nl, y) \quad n = -\infty, \dots, \infty$$

$$F_{n,1}(y) - F_{n,2}(y) = Gw_1(nl, y) \quad n = -\infty, \dots, \infty \quad (14)$$

where $G(\cdot)$ is a linear operator. $F_{1,n}$ and $F_{2,n}$ are the reaction forces acting on the first and second plate respectively.

Assume that the reaction pressures can be related to the displacements through linear operators. This implies that the spatial Fourier transform of each operator will be an algebraic expression. The operators and the corresponding Fourier transforms will be given in section 3.2. Script-typed symbols will denote the operators. Thus, the reaction pressures can be written as

$$p_r(x, y) = R w_1(x, y), \quad p_t(x, y) = T w_2(x, y), \quad (15 \text{ a,b})$$

$$p_{r1}(x, y) = \sum_{n=-\infty}^{\infty} F_{n,1}(y) \cdot \delta(x - nl), \quad p_{r2}(x, y) = \sum_{n=-\infty}^{\infty} F_{n,2}(y) \cdot \delta(x - nl), \quad (15 \text{ c,d})$$

$$\begin{bmatrix} p_c(x, y, 0) \\ p_c(x, y, d) \end{bmatrix} = \begin{bmatrix} j_{11} & j_{12} \\ j_{21} & j_{22} \end{bmatrix} \begin{bmatrix} w_1(x, y) \\ -w_2(x, y) \end{bmatrix}. \quad (15 \text{ e})$$

The transform of the sums in (15 c-d) can be written as,

$$F_{x,y} \sum_{n=-\infty}^{\infty} F_n(y) \cdot \delta(x - nl) = \sum_{n=-\infty}^{\infty} \tilde{F}_n(\beta) \cdot e^{i\alpha nl},$$

where $F_{x,y}(\cdot)$ indicates the Fourier transform operator (2 a) and the force field is only transformed in the y -direction. Here, Lin and Garrellick [8] assume that the force function is two-dimensional, and then using the same form of expression as for the sum of the displacement field derived below. Their result seems to be accurate it is unnecessary to intrude this somewhat doubtful assumption.

The Poisson's sum can be used to show that

$$\sum_{n=-\infty}^{\infty} e^{i\alpha nl} = 2\pi \sum_{n=-\infty}^{\infty} \delta(\alpha l - 2n\pi). \quad (16)$$

The transform of the sum over the displacement points can then after some manipulations, using (16), be written as [1, 7]

$$F_{x,y} \sum_{n=-\infty}^{\infty} w(nl, y) \cdot \delta(x - nl) = \frac{1}{l} \cdot \sum_{n=-\infty}^{\infty} \tilde{w}\left(\alpha - \frac{2n\pi}{l}, \beta\right). \quad (17)$$

Transforming the pressures (15 a-f) gives algebraic expressions for the reaction pressures, and those can be written as

$$\tilde{p}_r(\alpha, \beta) = R \tilde{w}_1(\alpha, \beta), \quad \tilde{p}_t(\alpha, \beta) = T \tilde{w}_2(\alpha, \beta), \quad (18 \text{ a,b})$$

$$\tilde{p}_{r1}(\alpha, \beta) = \sum_{n=-\infty}^{\infty} \tilde{F}_{n,1}(\beta) \cdot e^{i\alpha nl}, \quad \tilde{p}_{r2}(\alpha, \beta) = \sum_{n=-\infty}^{\infty} \tilde{F}_{n,2}(\beta) \cdot e^{i\alpha nl}, \quad (18 \text{ c,d})$$

$$\begin{bmatrix} \tilde{p}_c(\alpha, \beta, 0) \\ \tilde{p}_c(\alpha, \beta, d) \end{bmatrix} = \begin{bmatrix} J_{11} & J_{12} \\ J_{21} & J_{22} \end{bmatrix} \begin{bmatrix} \tilde{w}_1(\alpha, \beta) \\ -\tilde{w}_2(\alpha, \beta) \end{bmatrix}. \quad (18 \text{ e})$$

Apply the Fourier transform to equation (12). Introduce two spatial dynamic stiffnesses

$$S_1(\alpha, \beta) = D_1(\alpha^2 + \beta^2)^2 - m_1^* \omega^2, \quad S_2(\alpha, \beta) = D_2(\alpha^2 + \beta^2)^2 - m_2^* \omega^2.$$

The transformed equation can now be rewritten in a matrix form, using (11) and suppressing the α and β dependence where not needed,

$$\begin{bmatrix} S_1 - R + J_{11} & -J_{12} \\ -J_{21} & S_2 + T + J_{22} \end{bmatrix} \begin{bmatrix} \tilde{w}_1 \\ \tilde{w}_2 \end{bmatrix} = \begin{bmatrix} \tilde{p}_e \\ 0 \end{bmatrix} - \sum_{n=-\infty}^{\infty} \begin{bmatrix} \tilde{F}_{n,1}(\beta) \cdot e^{ianl} \\ -\tilde{F}_{n,2}(\beta) \cdot e^{ianl} \end{bmatrix}. \quad (19)$$

Denote the first matrix from the left \mathbf{S} . Inverting \mathbf{S} and multiplying from the left yield the transformed displacements. In order to find a solution for the transformed displacement, the relations between the displacement and the force field in the beams has to be used. Define two help matrices \mathbf{P} , size 2×1 , and \mathbf{Y} , size 2×2 ,

$$\mathbf{P} = \sum_{n=-\infty}^{\infty} \mathbf{S}^{-1}(\alpha - en) \cdot \begin{bmatrix} \tilde{p}_e(\alpha - en) \\ 0 \end{bmatrix}, \quad \mathbf{Y} = \sum_{n=-\infty}^{\infty} \mathbf{S}^{-1}(\alpha - en), \quad (16a-b)$$

where $e=2\pi/l$. Equation (19) is now to be summed up at the position $\alpha=2\pi m/l=en$. In the first step, change variables to $\alpha=en$, where m is an integer. The statement $\exp(i\alpha n l + i e m n l) = \exp(i\alpha n l)$ can be used to suppress the m -dependence in the sum. In the second step, sum over all m 's and then let $m=n$,

$$\sum_{n=-\infty}^{\infty} \begin{bmatrix} \tilde{w}_1(\alpha - en) \\ \tilde{w}_2(\alpha - en) \end{bmatrix} = \begin{bmatrix} P_1 \\ P_2 \end{bmatrix} - \begin{bmatrix} Y_{11} & Y_{12} \\ Y_{21} & Y_{22} \end{bmatrix} \sum_{n=-\infty}^{\infty} \begin{bmatrix} \tilde{F}_{n,1}(\beta) \cdot e^{ianl} \\ -\tilde{F}_{n,2}(\beta) \cdot e^{ianl} \end{bmatrix}, \quad (18)$$

where the matrix components of (16) are written out. Solve for two of the infinite sums using the boundary conditions in (18). Combine this result with the summed and transformed boundary condition, yielding four unknown and four equations. The summed displacement is solved for, giving two remaining equations for the summed forces. Solving for the summed forces yields

$$\begin{cases} \sum_{n=-\infty}^{\infty} \tilde{F}_{n,2} \cdot e^{ianl} = \left(\frac{GP_2}{l + Y_{21}G} - \frac{GP_1}{l + Y_{11}G} \right) \left(\frac{Y_{12}G + l}{l + Y_{11}G} - \frac{Y_{22}G + l}{l + Y_{21}G} \right)^{-1} \\ \sum_{n=-\infty}^{\infty} \tilde{F}_{n,1} \cdot e^{ianl} = \left(\frac{GP_1}{l + Y_{12}G} - \frac{GP_2}{l + Y_{22}G} \right) \left(\frac{Y_{11}G + l}{l + Y_{12}G} - \frac{Y_{21}G + l}{l + Y_{22}G} \right)^{-1} \end{cases} \quad (20 \text{ b})$$

And finally is the solution found.

3.2 THE EXCITATION AND REACTION FORCES

The excitation force is assumed to be a point force in the position x_0, y_0 , $p_e(x, y) = F_R \delta(x - x_0, y - y_0)$, where F_R is the time-frequency Fourier transform of the excitation force of the impact under consideration, and subscript R stands for repeated signals. The corresponding spatial Fourier transform (2 a) is

$$\tilde{p}_e(\alpha, \beta) = F_R e^{i(\alpha x_0 + \beta y_0)}. \quad (23 \text{ b})$$

F_R is specified in section 2.

For the n 'th frame, the equation of motion, modelled as a Euler beam and excited by a linear force $Q_n(y)$ along the line $x = nl$, is

$$E_I I_f \frac{d^4 u_n}{dy^4} - \rho_f A_f \omega^2 u_n = Q_n, \quad (24 \text{ a})$$

where $E_f l_f$ is the bending rigidity and $\rho_f A_f$ is mass per unit length of the frame. The difference between the plates as regards frame reaction pressure is

$$p_{f1}(x, y) - p_{f2}(x, y) = \sum_{n=-\infty}^{\infty} \left(E_f l_f \frac{d^4 u_n}{dy^4} - \rho_f A_f \omega^2 u_n \right) \delta(x - nl). \quad (23)$$

From equation (22) the operator G in equation (14) can now be identified. Thus, the algebraic expression for G is found by transforming (23), $G = E_f l_f \beta^4 - \rho_f A_f \omega^2$.

Consider a fluid is occupying the upper half space with an acoustic pressure $p(x, y, z)$, $z \leq 0$, and the lower half space is occupied by a fluid with a acoustic pressure $p(x, y, z)$, $z \geq d$. It is assumed that the two fields have the same sound speed c_0 and density ρ_0 . Two moving surfaces are occupying the x - y -plane in $z=0$ and $z=d$, vibrating with displacements $w_1(x, y)$ and $w_2(x, y)$. The acoustic pressure satisfies the Helmholtz equation together with the boundary conditions

$$\left[\frac{\partial p_i}{\partial z} \right]_{z=0} = \omega^2 \rho_0 w_1, \quad \left[\frac{\partial p_i}{\partial z} \right]_{z=d} = \omega^2 \rho_0 w_2, \quad (24)$$

ensuring equality of the fluid velocity at the plate surface and the plate velocity. These equations corresponds to equations (14 a-b). The Helmholtz equation is now transformed, indicating a wave in the z -direction. The solution can be written as outgoing waves. Therefore, if $z=0$ and $z=d$ respectively,

$$\tilde{p}_r(\alpha, \beta, 0) = \frac{\omega^2 \rho \cdot \tilde{w}_1(\alpha, \beta)}{\sqrt{\alpha^2 + \beta^2 - k^2}}, \quad \tilde{p}_r(\alpha, \beta, d) = - \frac{\omega^2 \rho \cdot \tilde{w}_2(\alpha, \beta)}{\sqrt{\alpha^2 + \beta^2 - k^2}} \quad (25)$$

Hence, we can identify the coefficients in (11 a-b).

A fluid is also occupying the space $0 < z < d$. An acoustic pressure $p_c(x, y, z)$ is present. The acoustic pressure satisfies the Helmholtz equation where c_c is the speed of sound in the medium and ρ_c is the density. The acoustic pressure also satisfies the boundary conditions,

$$\left[\frac{\partial p_c}{\partial z} \right]_{z=0} = \omega^2 \rho_c w_1, \quad \left[\frac{\partial p_c}{\partial z} \right]_{z=d} = \omega^2 \rho_c w_2, \quad (26)$$

The Helmholtz equation is now transformed and a solution is found by assuming one wave in the positive z -direction and one in the negative z -direction. One derivation with respect to z gives an expression suited for the boundary condition. The amplitudes of the components in the standing wave are then obtained, using (26). After some manipulations, putting $z=0$ and $z=d$ respectively, and written in a matrix form the result reads

$$\begin{bmatrix} \tilde{p}_c(\alpha, \beta, 0) \\ \tilde{p}_c(\alpha, \beta, d) \end{bmatrix} = \frac{\omega^2 \rho_c}{k_c} \begin{bmatrix} \cot(k_c d) & \csc(k_c d) \\ \csc(k_c d) & \cot(k_c d) \end{bmatrix} \begin{bmatrix} \tilde{w}_1(\alpha, \beta) \\ -\tilde{w}_2(\alpha, \beta) \end{bmatrix}, \quad k_c = \sqrt{k_c^2 - \alpha^2 - \beta^2}, \quad (27)$$

where J_{11} , J_{12} , J_{21} and J_{22} in equation (18 e) can be identified respectively.

If the cavity is filled with mineral wool, a semi-empirical model of an equivalent fluid, formulated by Delaney and Bazley [10] can be used to derive the wavenumber k_{min} and the impedance z_{min} to be used. The flow resistance R_{min} of the mineral wool is the only material parameter for the mineral wool that is included in this model. The wavenumber k and characteristic impedance ρc is then replaced by $k_{c,min}$ and $z_{c,min}$ respectively.

4. THE RESPONSE

In order to compare the calculations with measured values, we now focus on the radiated powers. The finite area of radiation will probably effect the result but is not considered here. Instead the expression for power radiation found in Cremer and Heckl [3] will be used. In order to simplify the integration, use $\alpha = k \sin(\varphi)$ and $\beta = k \cos(\varphi)$ so that $d\alpha d\beta = k dk d\varphi$,

$$\Pi_{Rad} = \frac{k\rho c}{8\pi^2} \int_0^{2\pi} \int_0^\pi \frac{k^2 \omega^2 |\tilde{w}(k_r \sin(\varphi), k_r \cos(\varphi))|^2}{\sqrt{k^2 - k_r^2}} k_r dk_r d\varphi, \quad L_n = 10 \log \left(\frac{\Pi_{in}}{p_{ref}^2} \frac{4\rho c}{A_0} \right) \quad (28)$$

Equation (28) will be integrated numerically. The second expression, L_n being the impact noise level, is found by means of a power balance.

5. RESULTS

As an example of the prediction model Figure 4 is shown.

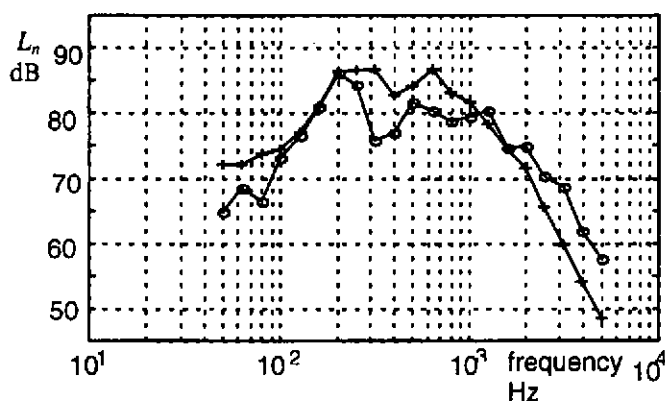


Figure 4 Floor with mineral wool. Mean over 15 positions, '+' measurements and 'o' calculations

6. REFERENCES

- 1 BRUNSKOG, J and HAMMER, P. 'Prediction of impact sound transmission of lightweight floors', Engineering Acoustics, LTH, Lund University, TVBA-3105, Sweden, 1999.
- 2 BRUNSKOG, J. and HAMMER, P., 'Prediction of impact noise of lightweight floors, including the tapping machine' *Proceedings of Inter-Noise 99*, Fort Lauderdale, Florida, pp 347--352, 1999
- 3 CREMER, L., HECKL, M. and UNGAR, E. E., *Structure-Borne Sound*, Berlin: Springer-Verlag, second edition, 1988, 1973.
- 4 LINDBLAD, S., 'Impact Sound characteristics of resilient floor coverings. A study on linear and nonlinear dissipative compliance'. Div. Building Technology, LTH, Bulletin 2, Lund, Sweden, 1968.
- 5 VÉR, I. L., 'Impact Noise Isolation of Composite Floors', *J. Acoust. Soc. of Amer.* **50** (4), pp 1043-1050, 1971.
- 6 TIMOSHENKO, S., *Theory of Elasticity*, 333-344, McGraw-Hill, New York and London, 1939.
- 7 MACE, B. R. 'Sound radiate from a plate reinforced by two sets of parallel stiffeners' *J. Sound Vib.* **71** (3), pp 435-441, 1980.
- 8 LIN, G. F. and GARRELICK, J. M. 'Sound transmission through periodically framed parallel plates', *J. Acoust. Soc. of Amer.* **61** (4), 1014-1018, 1977.
- 9 TAKAHASHI, D., 'Sound radiated from periodically connected double-plate structures', *J. Sound Vib.* **90** (4), 541-557, 1983.
- 10 DELANEY, M. E. and BAZELY, E. N. 'Acoustical properties of fibrous absorbent materials' *Appl. Acoust.* **3**, 105-116, 1970.